PHYSICAL REVIEW B VOLUME 27, NUMBER 10 15 MAY 1983

Dynamical exchange and correlation effects in photoemission from metals

P. O. Nilsson and C. G. Larsson
Department of Physics, Chalmers University of Technology, S-412 96 Göteborg, Sweden
(Received 28 July 1982)

A muffin-tin potential for metals in the photoexcited state has been constructed with the use of an approximation for exchange and correlation in the electron gas by Hedin and Lundqvist. This potential has been included in calculations of the photocurrent. The dynamical effects so included have been studied in detail for the case of Cu.

I. INTRODUCTION

In the present paper we are concerned with the description of the excited state in photoemission. In the past ten years a number of papers have been devoted to the theory of photoemission (see, e.g., Refs. 1—4). The conclusion has been made that simple theoretical models work well for comparison with experimental photoelectron energies. The single-particle approximation has, in spite of the neglect of complex electron and hole interactions, produced very accurate results. For instance, photoemission experiments have been used as a test of E-vs-k relations and the agreement with ground-state band-structure calculations has been quite good. The conclusion from such studies has been that the simple theoretical model which has been applied together with a specific ground-state band structure describes in practice the photoemission process with sufficient accuracy.

In recent years this situation has changed slightly. As experimental techniques have improved, and band-structure calculations have become more sophisticated, differences between experimental and theoretical results have become more clear. Different band-structure calculational methods give quite similar results, but there still exists a certain spread among the reported eigenvalues. Moreover, as has been noted, for example, by Courths *et al.*[5] in the case of Cu, the differences between the experimental and the theoretical values often have the same sign for a given $\vec{k}$ point. Systematic differences of this kind were discussed by Wagner *et al.*[6] and were suggested to be effects of the final state in the photoemission process. Empirical corrections to the ground-state band structure have accordingly been carried out[7,8] in order to increase the agreement with experimental data. There are also some calculations in the literature[9—11] on the effects of an excitation potential, based on fundamental work on the electron gas by Sham and Kohn.[12] To our knowledge there exists, however, no *ab initio* photoemission calculation in which dynamical exchange and correlation effects in the final state have been included. This is the goal of the present paper.

The mathematical description we use for the photoemission process is given in Sec. II. In Sec. III the construction of the dynamical exchange-correlation potential is sketched. Technical details are given in the Appendix. Section IV presents the results obtained and comparisons with experimental data are made. In Sec. V we analyze the various calculational steps in some detail. Finally we give, in Sec. VI, some conclusions and suggestions for future work.

II. THE PHOTOEMISSION PROCESS

Several authors have given complete descriptions of the photoemission process in the noninteracting case.[2—4] We will here follow the formulation given by Caroli *et al.*[4] and by Pendry.[13] In their description the photocurrent is written as

$$I=\frac{1}{\pi}\mathrm{Im}\langle\phi\,|\,G_2^{+}\Delta G_1^{+}\Delta^{+}G_2^{-}\,|\,\phi\rangle\ . \tag{1}$$

Here $G_{1,2}$ are the hole and electron Green's functions, respectively, and Δ is the photon-field operator. This formula is valid if one neglects quantum-mechanical interference terms and terms representing inelastic energy losses. The simplest approximation, the noninteracting single-particle approximation, is illustrated in Fig. 1(a). This can be extended in different ways by including various interactions in the formalism.[4] In the present work we have included effects to the electron and hole Green's functions due to dynamic exchange and correlation in the electron gas. This is realized by separate renormalizations of the propagators G_{0a} ($a=1$ or 2) of Fig. 1(a). The renormalized, one-particle propagators (quasiparticles) G_a can be obtained from the ground-state propagators via the Dyson equation [see Figs. 1(b) and 1(c)]. Interactions of the medium with the escaping electron and the remaining hole are in this way taken into account by the use of a

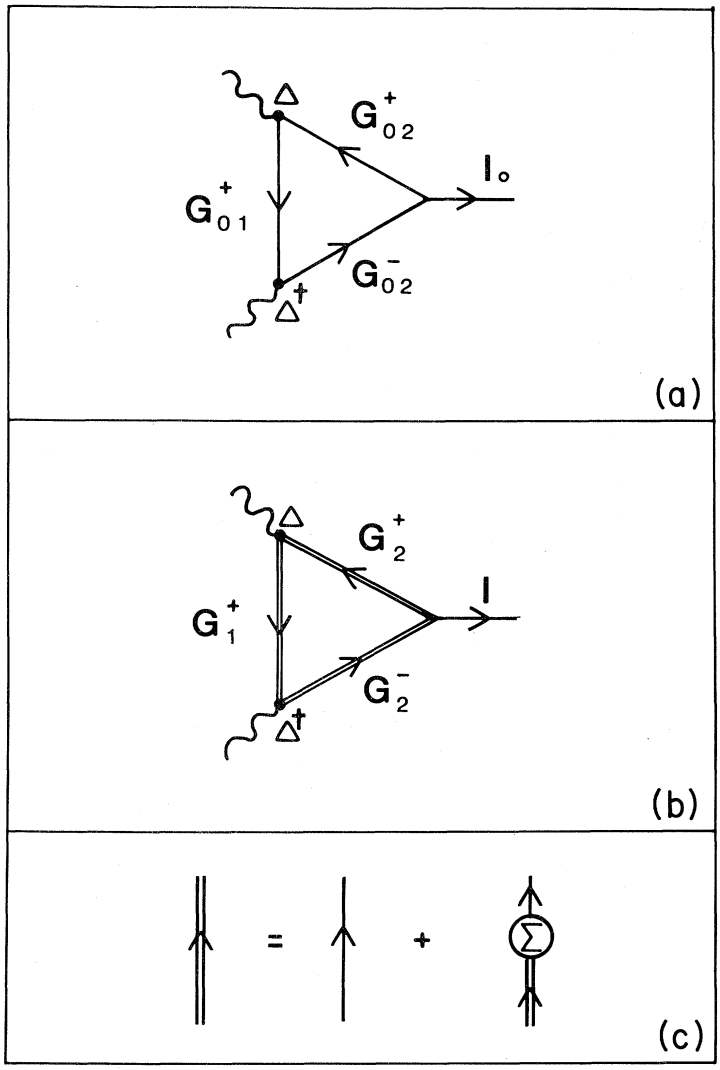

FIG. 1. (a) Diagrammatic representation of the photoemission current in lowest order (noninteracting case). Compare Eq. (1). (b) Same diagram as in (a), but with renormalized propagators. (c) Dyson equation for the renormalized propagator in (b). The self-energy Σ is represented in the present work by the Hedin-Lundqvist random-phase—approximation (RPA) exchange-correlation function (Refs. 15 and 16).

self-energy, or optical potential. The imaginary part of this potential corresponds to real excitations and describes the absorption of the electron and hole flux. The real part is usually neglected in the literature, or taken to be a constant. It corresponds to virtual excitations and causes shifts of the energy levels. The purpose of the present paper is to include a more realistic description of this effect. As will be seen in Sec. III the specific numerical approximations we apply for the self-energy reduce the problem to the introduction of a local, but energy-dependent, potential. This potential can be fairly easily incorporated in a computing scheme which has already been established for calculation of the photocurrent.[14]

Although many approximations have been introduced above we believe that our computational results take into account the essential corrections to the ground-state energy levels in metals as observed in photoelectron spectroscopy. The numerical agreement with experimental data can probably be increased further by improving some of the various approximations, e.g., in Σ and the ground-state calculation.

III. THE DYNAMICAL POTENTIAL

As mentioned above, two particles are of interest in photoemission, namely the photoelectron and the hole left behind. The photoelectron is represented by the so-called time-reversed—LEED (low-energy electron diffraction) state.[14] This means that we trace the electron from the detector into the crystal and find the appropriate state by a multiple-scattering calculation. This method is most compactly formulated using propagators. The Green's function for a noninteracting electron with energy E and momentum k in a homogeneous system can be written

$$G_0(k,E)=[E-\epsilon(k)-\mu_{xc}(\rho)+i\delta]^{-1} . \quad (2)$$

Here $\epsilon'(k)=\epsilon(k)+\mu_{xc}(\rho)$ is the eigenvalue of the ground-state Hamiltonian including exchange and correlation contributions to the ground state $\mu_{xc}(\rho)$. Multiple scattering can also be used to calculate the low-energy state, and an expression similar to Eq. (2) is used also for the hole. By combining these expressions, and the operator for the photon field, the photoemission formula can be written in the compact form of Eq. (1). Because of the neglect of damping effects, this scheme gives in practice the same eigenvalues as in a band-structure calculation.

When the interaction between the electron (hole) and the electron gas is turned on, there occur perturbations which change the properties of the final state. The sources of these effects are virtual and real excitations. These processes can be treated in the theory by including a self-energy in the Green's functions. In a homogeneous system the Green's function for the hole and electron state can then be written as

$$G(k,E)=[E-\epsilon(k)-\Sigma(\rho,E)+i\delta]^{-1} . \quad (3)$$

In general, Σ is a complex, nonlocal, energy-dependent function. Sham and Kohn[12] used the self-energy for the homogeneous electron gas Σ_h and applied the local-density approximation (LDA). Moreover, they introduced a local momentum leading to a local potential. This potential is, however, still energy dependent and complex. Lundqvist[15] and Hedin and Lundqvist[16] achieved numerical values for this potential by computations using a dynamically screened interaction expanded to lowest order. In Fig. 2 the results from Ref. 15 for the real and imaginary parts of Σ are shown. Similar electron-gas data from Ref. 16 will be used in the present work to represent the exchange-correlation part of the excitation potential for a real solid. We have not changed the real part in our calculations, but for computational reasons a simpler approximation has been made for the imaginary part. This will now be explained.

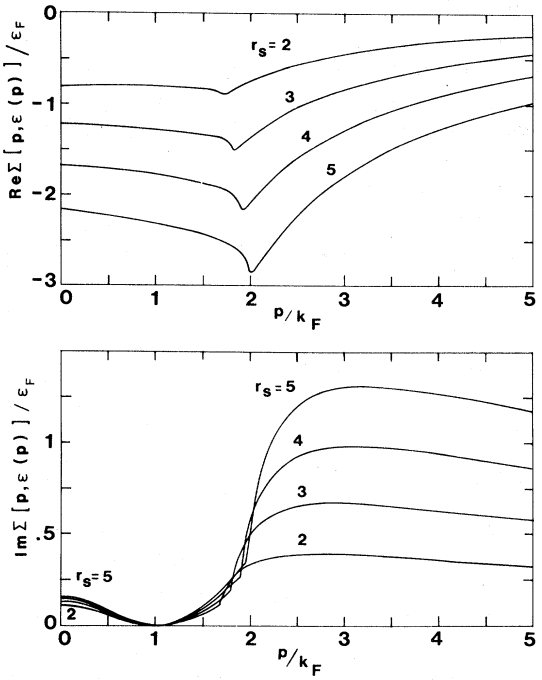

FIG. 2. Real and imaginary parts of the RPA self-energy as calculated by Lundqvist (Ref. 15). The self-energy numerically applied in the present work was slightly different (Ref. 16).

As can be seen in Fig. 2 the self-energy of an electron has a rather large imaginary part (i.e., it is strongly damped) as soon as the energy is high enough for plasmon creation to occur (10—20 eV). For many metals the plasmon is not a very well-defined quasiparticle. However, it is known that considerable dampling occurs for high energies. For the hole state the situation is different. Only Auger processes relatively close to the Fermi level affect its lifetime. Accordingly, this state will be sharper than the electron state which is also seen in photoemission experiments. For transition elements, which have unoccupied states of high density just above the Fermi level, the hole damping could still be appreciable. It is, however, less than the electron damping is at, for example approximately 50 eV above the Fermi level. From Fig. 2 we see that the use of two constants for ImΣ, one for each state, does not seem to be too crude an approximation (if not very low-photon energies are used). The size of the constants can be fitted to typical values of the electron density in the interstitial region between the individual muffin-tin spheres. This is the same procedure as suggested by Pendry.[13] Our approximation of constant damping is not at all important for the present study of energy levels.

The real part of the self-energy in Fig. 2 is given for an electron gas of constant density while we are using the muffin-tin—potential approximation. In the regions of the nonconstant part of the muffin-tin potential the density varies rapidly with the coordinate r, which is illustrated in Fig. 7(a). For a given radius r and energy E, $\rho(r)$ and $p(r)$ can be obtained. For these given values the self-energy $\Sigma(\rho,E,p)$ is calculated and we obtain the corresponding potential (LDA, Ref. 16)

$$V_{xc}(\rho,p)=\mathrm{Re}\Sigma(\rho(r),E,p)\ . \tag{4}$$

Including this effective exchange and correlation potential in Eq. (3) will give us a suitable expression for a photoemission calculation,

$$G'(k,E)=[E-E'(k)-iV_{0i}]^{-1}\ . \tag{5}$$

Here we have approximated the imaginary part of the self-energy with a constant. $E'(k)=\epsilon(k)+V_{xc}(\rho,p)$ is the eigenvalue of the Hamiltonian including the dynamic exchange and correlation potential V_{xc}. For further details see the Appendix.

It is important to notice that our calculations are based on the self-energy calculated for an electron gas, and used in the local-density approximation. Other types of many-body effects (for example, the two-hole correlation in Ni) can of course be included in the same manner in a photoemission calculation if only the appropriate self-energy is available.

IV. RESULTS

We have earlier reported[8,17] on small but significant energy differences between experimental photoemission data and ground-state band-structure calculations. We present here computational results for Cu(111), but we have also obtained similar results for other elements.[18]

In Fig. 3 we show the occupied part of the band structure of Cu in the Γ-L direction calculated with the photoemission program using zero damping $V_{0i}=0$. The dashed curve corresponds to a self-consistent ground-state potential.[19] The solid curve has been obtained with the excitation potential generated as described in Sec. III and the Appendix. We observe an increased binding energy for the d states of the order of 0.1 eV. This is similar to that which was reported in Ref. 11. The $l=2$ phase shift in Fig. 4 illustrates this downward shift of the d resonance. The s-p band is quite unaffected.

In Fig. 5 we show the corresponding photoelectron energy distribution curves (EDC) at 21.2-eV photon energy but with $V_{0i}\neq 0$. Again the dashed curve corresponds to the ground-state potential, while the solid-line curve has been obtained with the energy-dependent potential. The low binding-energy peak is found to shift 0.06 eV to a higher binding energy, while the other two peaks move 0.09 eV in the same direction. These peak shifts correspond to approximately a 2.5% change in binding energy. The vertical lines show the positions of the experimentally observed peaks.[17] Obviously, the differences between theoretical and experimental results decrease somewhat by the use of the energy-dependent potential, but there is still a discrepancy

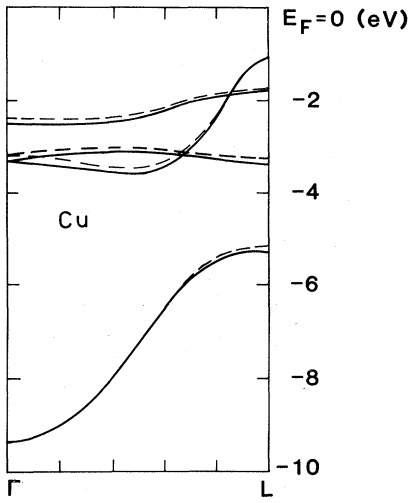

FIG. 3. Calculated occupied energy bands in the Γ-L direction for Cu. The dashed bands derive from a ground-state potential (Ref. 19) and the solid lines from an energy-dependent excitation potential [Eq. (A9)].

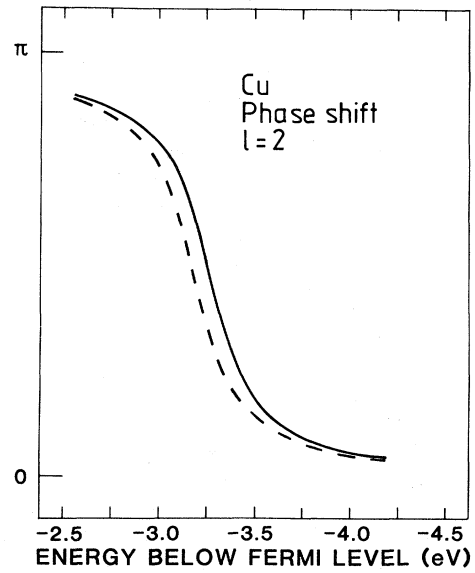

FIG. 4. $l=2$ phase shift for the two potentials used for Fig. 3.

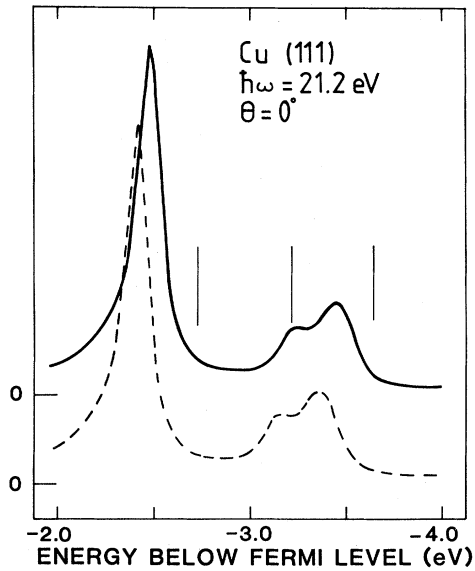

FIG. 5. Calculated photoemission EDC for Cu. The dashed curve corresponds to a ground-state potential (Ref. 19) and the solid-line curve to the energy-dependent excitation potential [Eq. (A9)]. The bars show the experimentally obtained peak positions (Ref. 8).

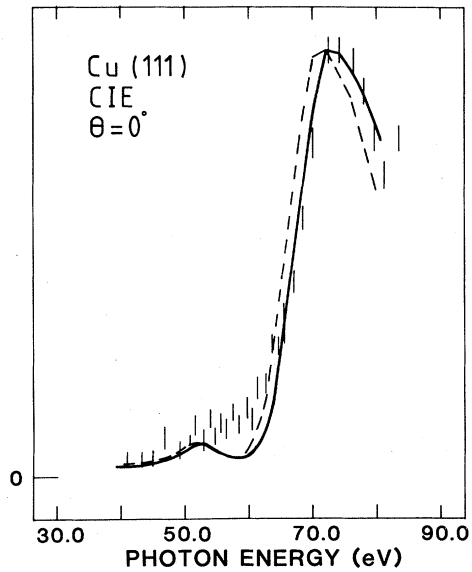

FIG. 6. Calculated CIEC for normal photoemission from Cu(111). The dashed curve corresponds to the ground-state potential and an initial energy of 5.28 eV below the Fermi level (E_F). The solid-line curve is calculated using the excitation potential with an initial energy of 5.41 eV below E_F. Both curves correspond to emission from the top, flat part of the d subband close to the L point. The bars are the experimental results from Ref. 21.

which remains.

For investigations of the self-energy effect on the photoelectron we have extended the EDC calculations to higher photon energies. We observe strong modulations in the peak amplitudes of the EDC as a function of photon energy. In particular, the peak around 5-eV binding energy goes through a maximum around 70-eV photon energy. Such modulations have been observed experimentally.[20,21] In Fig. 6 the amplitude variation of the 5-eV peak is plotted as a function of photon energy [constant—initial-energy curve (CIEC)]. As can be seen, the self-energy correction brings theory in better agreement with experiment. We have earlier identified[17,22] the observed peak as an interband resonance corresponding to transitions from a flat d subband into a broad free-electron band at the L point, rather than as emission from a surface state.[21] This mechanism is in principle the same as in x-ray-absorption near-edge structure (XANES) experiments. The peak position at 73 eV can thus be correlated with the lattice constant of Cu.

V. DISCUSSION

From the preceeding section it is clear that the use of an excitation potential improves the agreement between experimental and theoretical photoelectron energies. The discrepancy which remains may to some degree originate from uncertainties in the ground-state potential. However, we believe that the main effect originates from approximations in the excitation potential, at least with regard to the high-energy (electron) state. To discuss this in some detail we will now analyze the various steps of the computational results presented above.

The starting point was a self-energy of the type shown in Fig. 2. This has been obtained[15,16] by a lowest-order calculation on the homogeneous electron gas. From a computational point of view there are two contributions to the dynamical potential, as is evident from Eq. (A9): the correction of the muffin-tin (MT) potential and the correction of the MT zero in the interstitial region. In order to obtain numerical values for the first term, the electron-gas data in Fig. 2 for the real part of the self-energy is extended to lower r_s values in Fig. 7(a) (broken lines). The solution of Eq. (A5) in the Appendix for the Cu MT potential is shown as solid lines in the same figure for a few energies. Figure 7(b) displays the same data, but normalized to the value at the Fermi energy. The actual MT-potential correction is shown in Fig. 8 for a few energies. Figure 9 shows the energy dependence of the MT zero for the dynamical potential [last term of Eq. (A9)]. The actual photoemission calculation is performed with the two corrections of Figs. 8 and 9, respectively. The

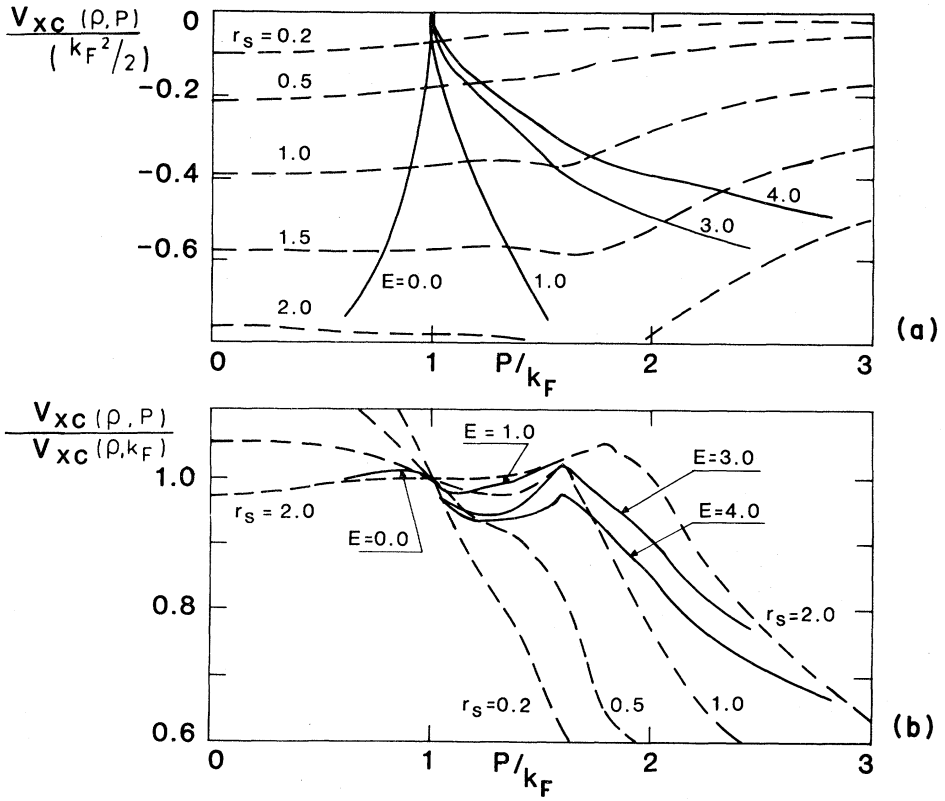

FIG. 7. (a) Dynamical exchange-correlation potential normalized to the electron-gas Fermi energy. The dashed lines are for typical electron densities in a metal. The solid lines correspond to the actual exchange-correlation potential for Cu at a few energies. (b) Same as for (a) but the potential is now normalized to its value on the Fermi surface.

eigenvalues in this manner are thereafter "corrected back" using Eq. (A10), i.e., the function of Fig. 9. Thus, a qualitative picture of the net effect is given in Fig. 8. We conclude that, although the electron-gas data of Fig. 7 could in principle give negative and positive corrections both above and below the Fermi level, real electron densities give a simpler picture. For normal densities the correction below

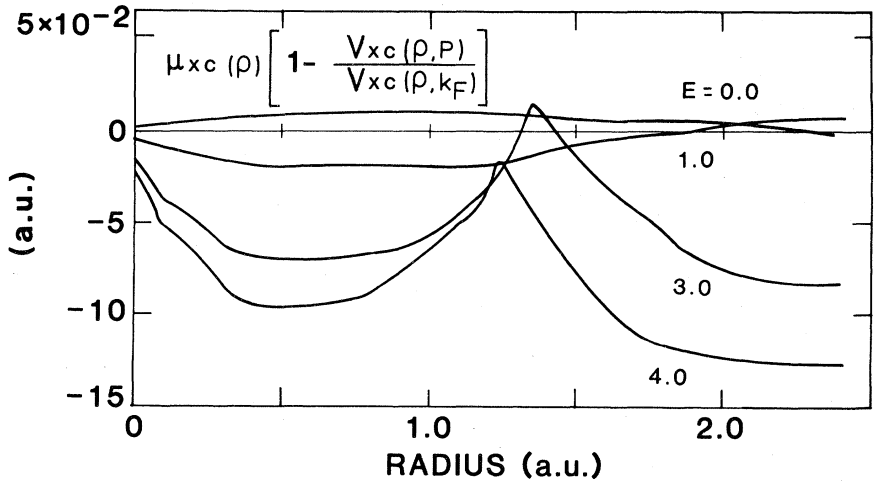

FIG. 8. Potential correction term as a function of radius for a few energies. The Fermi energy is 0.314 hartree. The peak around $r=1.4$ for $E=3.0$ and 4.0 hartree corresponds to the plasmon dip in the electron-gas function of Fig. 2.

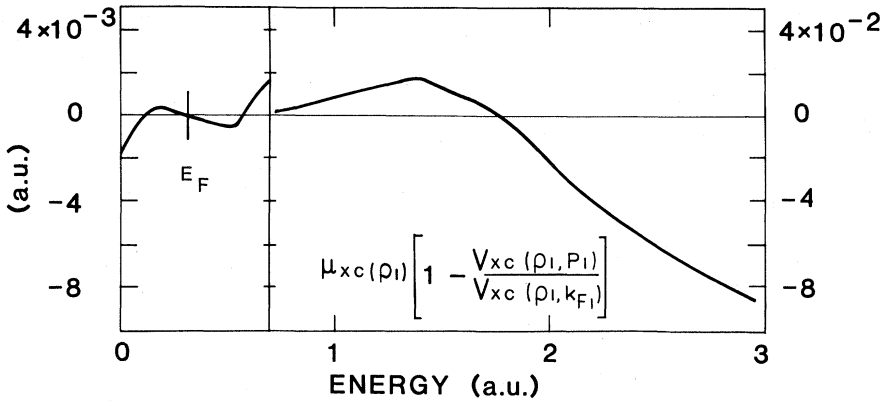

FIG. 9. Muffin-tin—zero correction to the potential [Eq. (A10)] as a function of energy. Note the different scales.

E_F will be negative, i.e., the dynamic potential is more attractive than the static one. This correction is, however, expected to be numerically small (0.1 eV). It is only for unrealistically large densities that an Hartree-Fock behavior is approached. The largest effect for Cu occurs around $r=1.2$ a.u., and this can be seen in Fig. 8 for $E=0$. The $3d$ states are heavily weighted in this region while the $4s$ and $4p$ states have their main contribution further out. Thus the finding in Fig. 3, that the $4s,p$ conduction band is rather unaffected, can be explained in this way.

Above the Fermi energy shifts become much larger in general. Of course, for very large energies the exchange-correlation forces must vanish completely. Thus a maximum shift equal to the static exchange-correlation energy is expected. For the electron density in the interstitial region ($r_s=2$) this corresponds to about 10 eV. However, for an electron gas this transition is not smooth. In particular, for low densities the strong plasmon interaction results in an abrupt increase in the imaginary part and accordingly a dip in the real part of the self-energy (see Fig. 2). This effect survives in the LDA calculations for Cu, as is evident from Figs. 7 and 8, and causes a delaying effect in the reduction of the self-energy as a function of quasiparticle energy. The reason why we only obtain about half (2 eV) of the required shift (4 eV) of the bands that are about 70 eV above E_F in Cu is likely to be due to the "plasmon delay" just described. The plasmon for Cu is in reality far from being as well defined as for the corresponding electron gas. We have found the same effect for Pd, where a shift of 4 eV was observed,[8] while we calculated about 2 eV.[18] Accordingly, the peaks of the functions in Fig. 7 should be smeared out, resulting in an effectively larger photoelectron shift for a given energy.

VI. CONCLUSIONS

Comparisons between experimental photoelectron energies (for a typical metal such as Cu) and corresponding ground-state band-structure calculations suggest that effects of the excited state (modified exchange and correlation) can be observed. For the holes in the valence band the effect is small (less than 0.1 eV) and of the order of the uncertainty in ground-state band structure calculations, but systematic. For the excited electron the effect becomes large at high energies (4 eV at 70 eV above E_F).

With the use of data for the self-energy of the electron and hole in the homogeneous electron gas a local but energy-dependent potential can be constructed (Ref. 16). Such a potential was applied in the present work for the calculation of photoelectron specta. Comparisons with experiment show improved agreement: About half of the wanted correction was achieved. The remaining descrepancy is probably due to the strong plasmon contribution in the homogeneous electron gas not present in most transition and noble metals.

To further investigate these phenomena we suggest two studies. Firstly, typical free-electron metals such as aluminum should be studied experimentally and comparisons should be made with the present theory. Secondly, efforts should be done to improve on the self-energy data, e.g., by using a more realistic screening (dielectric) function in the case of non-free-electron solids.

ACKNOWLEDGMENTS

Financial support from the Swedish Natural Science Research Council is gratefully acknowledged. We would also like to thank U. Barth, L. Hedin, and B. Lundqvist for valuable discussions.

APPENDIX

As mentioned in Sec. III, Sham and Kohn[12] proposed a local approximation for the density and for the momentum. This leads to a local, but energy-dependent, potential

$$V_{xc}(\rho,p)=\mathrm{Re}\Sigma_h(\rho(r),E,p)\ . \tag{A1}$$

The energy of the quasiparticle can thus be written as

$$E(p,\rho)=p^2/2+V_{xc}(\rho,p)\ , \tag{A2}$$

To determine the local momentum $p(r)$, Sham and Kohn proposed[12] two alternatives. We have used the following:

$$E(p,\rho)=E_k-E_F+\mu_k(\rho)\ . \tag{A3}$$

This procedure has been analyzed by Hedin and Lundqvist.[16] E_k is the excitation energy relative the Fermi level E_F and μ_k is the chemical potential for the ground state of homogeneous electron gas:

$$\mu_k(\rho)=\tfrac{1}{2}k_F^2+\mu_{xc}(\rho)\ . \tag{A4}$$

Combining Eqs. (A2)—(A4) gives

$$\tfrac{1}{2}p=E_k-E_F+\tfrac{1}{2}k_F^2+\mu_{xc}(\rho)-V_{xc}(\rho,p)\ . \tag{A5}$$

Given the ground-state density $\rho(r)$ and a table for $V_{xc}(\rho,p)$, one can obviously determine $p(r)$ iteratively from Eq. (A5), and thus the local potential in Eq. (A1).

In the present case we have used a MT potential[19] which for the ground state can be written as

$$V_g(r)=V_{at}(r)+\mu_{xc}(\rho(r))-\mu_{xc}(\rho_I)\ . \tag{A6}$$

Here ρ_I is the density in the interstitial region and $V_{at}(r)$ the Hartree contribution to the potential. Correspondingly, we write for the excitation potential

$$V_e(r,E)=V_{at}(r)+V_{xc}(\rho(r),p)-V_{xc}(\rho_I,p_I)\ . \tag{A7}$$

To avoid unphysical effects at the Fermi energy we force the two potentials to be equal at the Fermi energy:

$$V_g(r)=V_e(r,E_F)\ . \tag{A8}$$

Thus we finally arrive at the excitation potential used in the present work:

$$V_e(r,E)=V_g(r)-\mu_{xc}(\rho(r))\times\left[1-\frac{V_{xc}(\rho(r),p)}{V_{xc}(\rho(r),k_F)}\right]+\mu_{xc}(\rho_I)\left[1-\frac{V_{xc}(\rho_I,p_I)}{V_{xc}(\rho_I,k_{FI})}\right]\ . \tag{A9}$$

Note that to calculate $p(r)$ for use in Eq. (A9) we have to modify Eq. (A5) using the criterion (A8). The interstitial density ρ_I was obtained from the number of electrons in the interstitial region as given in Ref. 19. The quasiparticle energy E_K (the measured energy) is related to the single-particle energy ϵ (used in the calculations) via

$$\epsilon=E_K+\mu_{xc}(\rho_I)\left[1-\frac{V_{xc}(\rho_I,p_I)}{V_{xc}(\rho_I,k_{FI})}\right]\ . \tag{A10}$$

[1] I. Adawi, Phys. Rev. 134, A788 (1964).
[2] G. D. Mahan, Phys. Rev. B 2, 4334 (1970).
[3] W. S. Schaich and N. W. Ashcroft, Phys. Rev. B 3, 2452 (1971).
[4] C. Caroli, D. Lederer-Rozenblatt, B. Roulet, and D. Saint-James, Phys. Rev. B 8, 4552 (1973).
[5] R. Courths, V. Bachlier, B. Cord, and S. Hüfner, Solid State Commun. 40, 1059 (1981).
[6] L. F. Wagner, W. E. Spicer, and S. Doniach, Solid State Commun. 15, 669 (1974).
[7] J. F. Janak, A. R. Williams, and V. L. Moruzzi, Phys. Rev. B 11, 1522 (1975).
[8] P. O. Nilsson, C. G. Larsson, and W. Eberhardt, Phys. Rev. B 24, 1739 (1981).
[9] L. Dagens and F. Perrot, Phys. Rev. B 8, 1281 (1973).
[10] G. Arbman and U. von Barth, Nuovo Cimento B 23, 37 (1974).
[11] R. E. Watson, J. F. Herbst, L. Hodges, B. I. Lundqvist, and J. W. Wilkins, Phys. Rev. B 13, 1463 (1976).
[12] L. J. Sham and W. Kohn, Phys. Rev. 14, 561 (1966).
[13] J. Pendry, Surf. Sci. 57, 679 (1976).
[14] J. F. L. Hopkinson, J. B. Pendry, and D. J. Titterington, Comput. Phys. Commun. 19, 69 (1980).
[15] B. I. Lundqvist, Phys. Status Solidi 32, 273 (1969).
[16] L. Hedin and B. I. Lundqvist, J. Phys. C 4, 2064 (1971).
[17] P. O. Nilsson, J. Kanski, and C. G. Larsson, Solid State Commun. 36, 111 (1980).
[18] C. G. Larsson and P. O. Nilsson (unpublished).
[19] V. L. Moruzzi, J. F. Janak, and A. R. Williams, *Calculated Electronic Properties of Metals* (Pergamon, New York, 1978).
[20] J. Stöhr, G. Apai, P. S. Wehner, F. R. McFeely, R. S. Williams, and D. A. Shirley, Phys. Rev. B 14, 1544 (1976).

[21]S. G. Louie, P. Thiry, R. Pinchaux, Y. Petroff, D. Chandesris, and J. Lecante, Phys. Rev. Lett. 44, 549 (1980).

[22]P. O. Nilsson, J. Kanski, and C. G. Larsson, in *Extended Abstracts of the International Conference on Vacuum Radiation Physics, Charlottesville, 1980* (unpublished), Vol. I.